Specific proteolytic cleavage of agrin regulates maturation of the neuromuscular junction

Marc F. Bolliger[1,*], Andreas Zurlinden[1,2,*], Daniel Lüscher[1,*], Lukas Bütikofer[1], Olga Shakhova[1], Maura Francolini[3], Serguei V. Kozlov[1], Paolo Cinelli[1], Alexander Stephan[1], Andreas D. Kistler[1], Thomas Rülicke[4,‡], Pawel Pelczar[4], Birgit Ledermann[4], Guido Fumagalli[5], Sergio M. Gloor[1], Beat Kunz[1] and Peter Sonderegger[1,§]

[1]Department of Biochemistry, University of Zurich, 8057 Zurich, Switzerland
[2]Neurotune AG, 8952 Schlieren, Switzerland
[3]Department of Medical Pharmacology, University of Milan, 20129 Milan, Italy
[4]Institute of Laboratory Animal Science, University of Zurich, 8091 Zurich, Switzerland
[5]Department of Medicine and Public Health, University of Verona, 37134 Verona, Italy

*These authors contributed equally to this work
‡Present address: Vetmeduni Vienna, 1210 Vienna, Austria
§Author for correspondence (peter.sonderegger@bioc.uzh.ch)

Accepted 5 August 2010
Journal of Cell Science 123, 3944-3955

doi:10.1242/jcs.072090

Summary

During the initial stage of neuromuscular junction (NMJ) formation, nerve-derived agrin cooperates with muscle-autonomous mechanisms in the organization and stabilization of a plaque-like postsynaptic specialization at the site of nerve–muscle contact. Subsequent NMJ maturation to the characteristic pretzel-like appearance requires extensive structural reorganization. We found that the progress of plaque-to-pretzel maturation is regulated by agrin. Excessive cleavage of agrin via transgenic overexpression of an agrin-cleaving protease, neurotrypsin, in motoneurons resulted in excessive reorganizational activity of the NMJs, leading to rapid dispersal of the synaptic specialization. By contrast, expression of cleavage-resistant agrin in motoneurons slowed down NMJ remodeling and delayed NMJ maturation. Neurotrypsin, which is the sole agrin-cleaving protease in the CNS, was excluded as the physiological agrin-cleaving protease at the NMJ, because NMJ maturation was normal in neurotrypsin-deficient mice. Together, our analyses characterize agrin cleavage at its proteolytic α- and β-sites by an as-yet-unspecified protease as a regulatory access for relieving the agrin-dependent constraint on endplate reorganization during NMJ maturation.

Key words: Agrin, Neuromuscular junction, Neurotrypsin, Proteolysis, Synaptogenesis

Introduction

During the initial stage of neuromuscular junction (NMJ) formation, nerve-derived agrin cooperates with muscle-autonomous mechanisms in the formation and stabilization of a primitive postsynaptic specialization comprising clustered acetylcholine receptors (AChR) (Bezakova and Ruegg, 2003; Kummer et al., 2006; Lin et al., 2008; McMahan, 1990; Sanes and Lichtman, 2001). Further agrin-mediated differentiation of the postsynaptic apparatus initiates reciprocal signals to the presynaptic nerve, resulting in the cessation of motor axon growth and the maturation of the presynaptic terminal (Nguyen et al., 2000). During the following weeks, the plaque-like early NMJ transforms to the typical pretzel-like structure that is characteristic of the mature endplate (Desaki and Uehara, 1987; Marques et al., 2000; Sanes and Lichtman, 2001; Slater, 1982). During this process, the topography of the postsynaptic membrane changes from an initially flat and apparently homogenous area to a complicated invaginated structure with a compartmentalized molecular composition. Removal of components from the postsynaptic specialization results in plaques with a single receptor-free area, appearing as a perforation, and subsequently in plaques with multiple and enlarged perforations, and eventually in the complex pretzel-like mature NMJ.

Because the generation of receptor-free areas within the postsynaptic membrane appears to be a key feature of NMJ maturation, we wondered whether the NMJ-promoting and stabilizing function of agrin needs to be reduced during this period. We investigated the role of proteolytic processing of agrin at the NMJ, because we recently found that agrin is cleaved by the neuronal serine protease neurotrypsin at two specific, highly conserved sites, and that agrin cleavage results in the dissociation and solubilization of the NMJ-promoting C-terminal domain of agrin (Reif et al., 2007). Here we demonstrate a correlation between the extent of agrin cleavage and the rate of NMJ maturation. Intriguingly, neurotrypsin was excluded as the physiological agrin-cleaving protease in this process, because NMJ reorganization and maturation proceeded normally in neurotrypsin-deficient mice. Our analyses confirm the role of agrin as a NMJ stabilizer and characterize agrin cleavage at its α- and β-sites as a regulatory access for the control of endplate reorganization during NMJ maturation.

Results

Excessive expression of neurotrypsin in spinal motoneurons results in NMJ disassembly and nerve fiber outgrowth

We generated conditional transgenic mice overexpressing neurotrypsin in neurons under the control of the Thy1 promoter (Caroni, 1997). Between the promoter and the open reading frame of the neurotrypsin cDNA, a transcriptional stop sequence, flanked

by two *loxP* sequences, was inserted (supplementary material Figs S1, S2) (Sauer, 1998). For selective transgene activation in motoneurons, these mice were crossed with a mouse line expressing Cre recombinase under the control of the Hb9 promoter (supplementary material Fig. S3) (Yang et al., 2001). Hb9 is a transcription factor that is selectively and transiently expressed in precursors of motoneurons (Arber et al., 1999). In western blots of spinal cord homogenates of adult mice, neurotrypsin expression was two to five times that of wild-type mice (supplementary material Fig. S3). For a control, a catalytically inactive form of neurotrypsin, with a mutation of the active-site serine to an alanine, was overexpressed in mice using a conventional Thy1 cassette (supplementary material Fig. S1). Overexpression of neurotrypsin enhanced cleavage of agrin at both cleavage sites, resulting in an increase of agrin-90 in spinal cord homogenates (supplementary material Fig. S4). pThy1-Nt/pHb9-Cre double-transgenic mice overexpressing active neurotrypsin in motoneurons developed normally during the first two postnatal weeks, but then slightly lagged behind their normal littermates with regard to growth of body mass. Mice overexpressing catalytically inactive neurotrypsin were normal in all aspects.

We studied the effect of neurotrypsin overexpression on neuromuscular innervation of the diaphragm muscle in adult mice (Fig. 1). To analyze NMJs in the endplate band in conjunction with their motor nerves, we triple-stained diaphragms with antibodies against neurofilaments to visualize nerves (Fig. 1A–C), antibodies

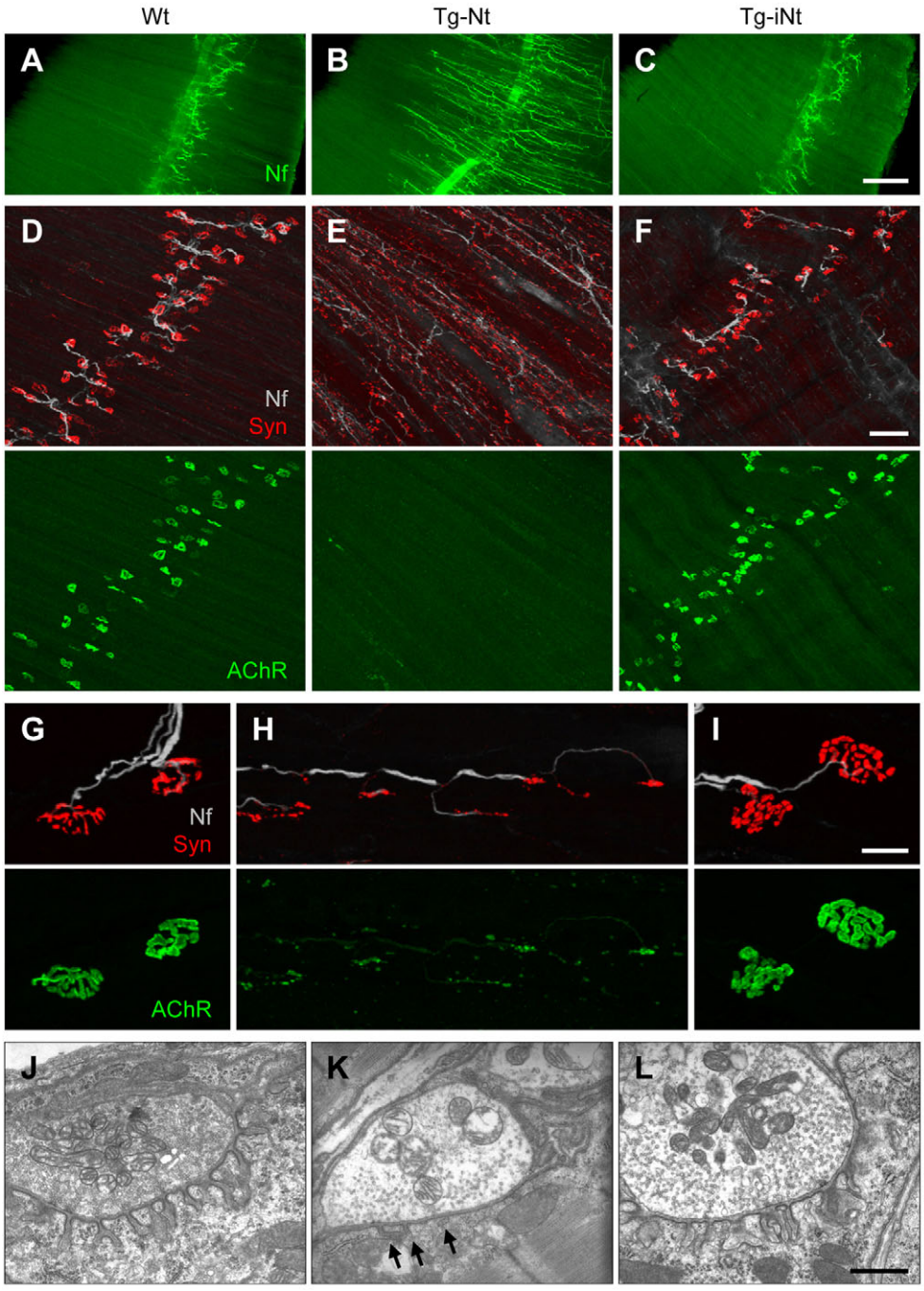

Fig. 1. Overexpression of neurotrypsin in motoneurons results in aberrant neuromuscular innervation. (**A–C**) Motor nerves innervating the diaphragm were visualized by neurofilament staining. (**D–I**) Neuromuscular innervation was visualized by triple-staining of neurofilament protein (Nf), synaptophysin (Syn), and acetylcholine receptor (AChR). Adult wild-type mice (A,D,G) were compared with mice overexpressing either active neurotrypsin (B,E,H) or inactive neurotrypsin (C,F,I). In adult neurotrypsin-overexpressing mice (B), motor axons grew out of the endplate band towards the medial and lateral borders of the hemidiaphragm. Innervation of muscles from mice overexpressing inactive neurotrypsin was normal (C). Normal NMJs in the endplate band were virtually absent in transgenic mice overexpressing active neurotrypsin (E). Staining for synaptophysin (E, upper panel) revealed many small, ectopic presynaptic boutons along the trajectories of outgrowing axons. No difference was seen between wild-type (D) and transgenic mice overexpressing inactive neurotrypsin (F). Ectopic AChR clusters in neurotrypsin-overexpressing mice were stained with considerably lower intensity (E, lower panel) and became detectable only after increasing the sensitivity of the microscope setting (H, lower panel). (**J–L**) Electron microscopy revealed that secondary folds of the postsynaptic membrane were absent or strongly reduced in number and depth in neurotrypsin-overexpressing mice (K, arrows point to folds). No difference was seen between wild-type mice (J) and mice overexpressing inactive neurotrypsin (L). Scale bars: 500 µm (C), 100 µm (F), 20 µm (I), and 1 µm (L). Wt, wild-type mice; Tg-Nt, transgenic mice overexpressing neurotrypsin; Tg-iNt, transgenic mice overexpressing inactive neurotrypsin.

against synaptophysin to visualize nerve terminals, and fluorophore-conjugated α-bungarotoxin to visualize AChR clusters of the postsynaptic apparatus (Fig. 1D–I). Overexpression of neurotrypsin in motoneurons severely altered neuromuscular innervation (Fig. 1B,E,H) compared with wild-type mice (Fig. 1A,D,G). Normally, nerves emerge from the central nerve bundle and innervate the muscle fibers within a short distance in the so-called endplate band (Fig. 1A). In neurotrypsin-overexpressing mice, nerves grew out past the normal sites of innervation and spread along the surface of the muscle fibers (Fig. 1B). Immunostaining for the presynaptic marker synaptophysin revealed numerous small speckles that were randomly distributed over the muscle, within and beyond the bounds of the endplate band (Fig. 1E, upper panel). Large postsynaptic specializations of the endplate band were almost completely absent, as demonstrated by stainings of AChRs with α-bungarotoxin (Fig. 1E, lower panel). Instead, small speckles with weak fluorescence intensity were found randomly distributed over the muscle surface. At higher magnification, the speckled staining for synaptophysin was found to be associated with en passant or terminal varicosities of diffusely grown motor nerves, most of them being colocalized with a small AChR cluster (Fig. 1H). This phenotype was only found in mice overexpressing catalytically active neurotrypsin, but not in mice overexpressing an inactive form of neurotrypsin (Fig. 1C,F,I), indicating increased proteolytic activity of neurotrypsin as the cause of the observed alterations.

Electron microscopic investigation of neurotrypsin-overexpressing mice showed that individual boutons (nerve terminals) were located at an unusually large distance from each other (tens of micrometers), whereas multiple boutons were found adjacent to each other in wild-type mice. Both in neurotrypsin-overexpressing mice (Fig. 1K) and in wild-type mice (Fig. 1J), the nerve endings were embedded in shallow depressions of the muscle fiber surface, the primary gutters. Most boutons were elliptical or round, although some with a longer and flat profile were also found. The largest diameters of the profiles were between 1 and 13 μm, with an average dimension of 4–5 μm. No statistically significant size difference between terminal boutons of wild-type and neurotrypsin-overexpressing mice was found. Similarly, the number of synaptic vesicles in presynaptic boutons was not significantly different in neurotrypsin-overexpressing mice compared with wild-type mice (data not shown). The synaptic cleft contained a contiguous basal lamina of normal thickness. No structural alterations reminiscent of membrane or extracellular matrix breakdown were seen. However, the postsynaptic apparatus of neurotrypsin-overexpressing mice was markedly reduced in complexity. Secondary folds were reduced in size and number or were completely absent (Fig. 1K), as confirmed by morphometric analysis (Table 1). No morphological alterations were found in mice overexpressing inactive neurotrypsin (Fig. 1L). The occurrence of single boutons, together with the virtual absence of secondary folds and the lower density of AChRs in the postsynaptic membrane, indicated that the synaptic structures of neurotrypsin-overexpressing mice corresponded to an early, immature stage of NMJ formation (Marques et al., 2000).

Table 1. Morphometric analysis of postsynaptic fold complexity

	n	Post-/presynaptic ratio
Wt	99	2.73±0.09
Tg-Nt	48	1.41±0.13
Tg-iNt	95	2.80±0.09

The ratio of postsynaptic versus presynaptic membrane length was determined and used as an estimate of the organization and complexity of the postsynaptic apparatus. Ratio values are mean ± s.e.m. The ratio for neurotrypsin-overexpressing mice (Tg-Nt) was significantly different ($P<0.001$, ANOVA with Tukey's post-hoc test) to that for wild-type mice (Wt) and for animals overexpressing catalytically inactive neurotrypsin (Tg-iNt).

NMJ disassembly occurs within days of elevation of neurotrypsin in motoneurons

To assess the time course of neurotrypsin-overexpression-induced changes at the NMJ, we studied the innervation of the diaphragm during the period of transgenic neurotrypsin upregulation. pThy1-driven transgenes were reported to reach full expression between postnatal days 6 (P6) and 10 (P10) (Caroni, 1997). Therefore, we double-stained diaphragms of wild-type (Fig. 2A,C,E) and neurotrypsin-overexpressing mice (Fig. 2B,D,F) on P0, P4 and P8 with antibodies against synaptophysin to visualize nerve terminals, and with α-bungarotoxin to visualize AChR clusters. At P0, we found a virtually identical pattern of the pre- and postsynaptic markers in wild-type (Fig. 2A) and neurotrypsin-overexpressing mice (Fig. 2B). In particular, all motor axons ended with a normally developed NMJ within the endplate band. No NMJs were located outside of the endplate band. By contrast, at P8, the majority of the NMJs in the endplate band had disappeared in neurotrypsin-overexpressing animals (Fig. 2F). The motor nerves had grown beyond the margins of the endplate band, and many small ectopic junctions had formed. At P4, a heterogeneous mixture of well-shaped and partially dissolved NMJs was found in the endplate band (Fig. 2D). The number of morphologically well-conserved NMJs was reduced by 50% compared with wild-type mice at P4 and neurotrypsin-overexpressing mice at P0. Small crumbled structures, stained intensively for both synaptophysin and AChR, were considerably more numerous than in wild-type mice. Most probably, they represented remnants of disappearing NMJs. Some motor axons had started to grow out and some had already crossed the borders of the endplate band. Thus, the endplate bands of P4 mice showed a transition state characterized by a combination of stages, including still well-conserved NMJs, structures reflecting a late stage of disassembly, and motor axons having resumed growth after complete disassembly of their endplates. To verify the temporal course of transgenic upregulation of neurotrypsin in motoneurons, we measured relative neurotrypsin levels in western blots of spinal cord homogenates of the same animals (Fig. 2G). We found that neurotrypsin overexpression at birth was at 40% of the full overexpression level, which was reached at P4 with approximately double the expression level of wild-type littermates. No further increase of neurotrypsin relative to wild-type animals was found at P8.

The electron microscopic analyses at P4 (Fig. 2H,I) and P10 (Fig. 2J,K) confirmed the striking transition resulting from the transgenic upregulation of neurotrypsin. At P4, when half of the NMJs had already been fully or partially disassembled, the remaining NMJs were structurally indistinguishable from those of wild-type mice (Fig. 2, compare H with I). In both cases, the presynaptic terminals were positioned on the flat surface of a muscle fiber or embedded in a shallow primary gutter. In some junctions, the formation of secondary folds had already begun, although this was not a general feature. By contrast, at P10, NMJs structurally corresponding to the expected developmental age were

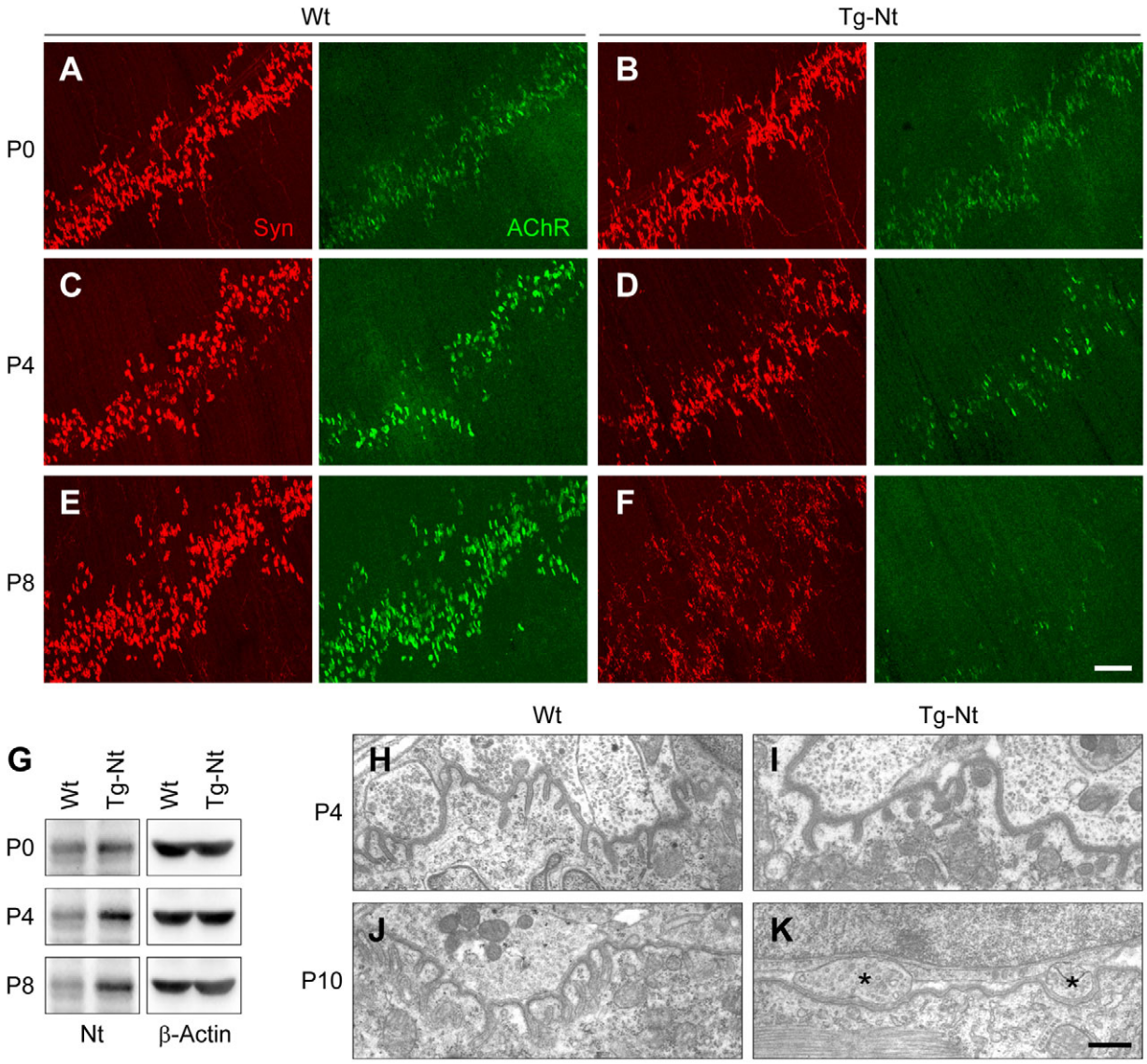

Fig. 2. Neurotrypsin overexpression in motoneurons disassembles previously formed NMJs within days. (**A**–**F**) Motor innervation of the diaphragm muscle was compared between wild-type mice (A,C,E) and neurotrypsin-overexpressing mice (B,D,F) during the period of transgenic neurotrypsin upregulation in motoneurons. Presynaptic nerve terminals and postsynaptic specializations were visualized by double-staining of synaptophysin (left panels, red) and AChRs (right panels, green), respectively. NMJ development proceeded properly before transgene activation. No difference between wild-type (A) and transgenic mice (B) was detected at P0. However, most NMJs disappeared within days after induction of neurotrypsin overexpression. At P8, the phenotype was fully established (F). At P4, a partial loss of NMJs indicates a transition stage with ongoing NMJ disassembly (D). (**G**) Immunoblots of spinal cord extracts taken from the same animals documented the rise of neurotrypsin (Nt) to full overexpression at P4. β-actin was used as a loading control. (**H**–**K**) Ultrastructural analysis demonstrated that the remaining endplates of neurotrypsin-overexpressing mice (I) were morphologically indistinguishable from those of wild-type littermates (H) at P4. Note that first secondary folds of the postsynaptic membrane had already been established in some of the NMJs. By contrast, at P10, comparing wild-type (J) with transgenic (K) mice only small, immature NMJs without secondary postsynaptic folds were found (marked by asterisks in K). Scale bars: 100 µm (F), and 0.5 µm (K). Wt, wild-type mice; Tg-Nt, transgenic mice overexpressing neurotrypsin.

only found in wild-type mice (Fig. 2J). Neurotrypsin-overexpressing mice had small, immature junctions, which characteristically had a well-established, contiguous basal lamina in the synaptic cleft, but no secondary folds in the postsynaptic membrane (Fig. 2K).

Together, these results indicate that transgenic elevation of neurotrypsin starts before birth and becomes maximal at around P4. The resulting disassembly of preexisting NMJs in the endplate band is at about midway at P4 and reaches completion around P8. Therefore, NMJs disassemble with a delay of a few days after transgenic upregulation of neurotrypsin.

Neurotrypsin-induced NMJ disassembly is preceded by precocious and accelerated NMJ maturation

The inspection of the remaining NMJs of neurotrypsin-overexpressing mice at P4 revealed plaques with multiple large, often confluent, perforations as well as pretzel-like structures (Fig. 3A–C). By their complex morphologies they were clearly distinct

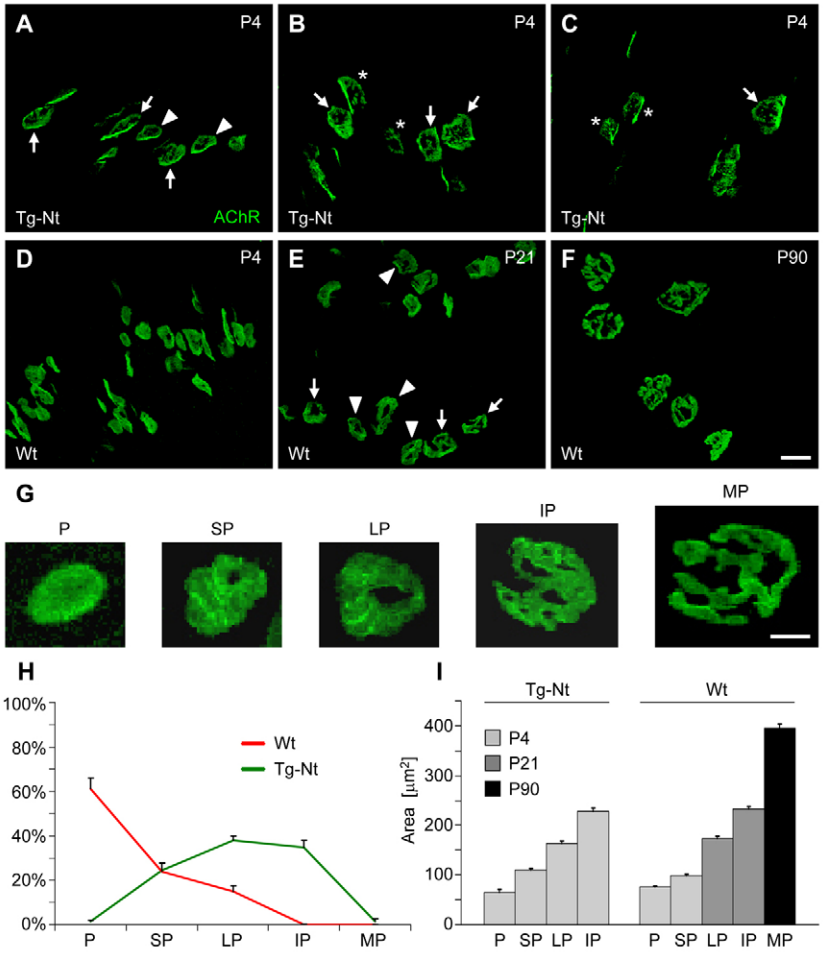

Fig. 3. NMJ disassembly in neurotrypsin-overexpressing mice is preceded by precocious and accelerated NMJ maturation. NMJs in the endplate band of the diaphragm of neurotrypsin-overexpressing and wild-type mice were stained with fluorescent α-bungarotoxin to label AChRs, and their maturational states were compared. (**A–C**) The number of morphologically intact NMJs in neurotrypsin-overexpressing mice at P4 was reduced to approximately 50%. Crumbled remnants (asterisks in B,C) indicated that many NMJs had reached a late stage of disassembly. The still relatively well-conserved NMJs exhibited large, often confluent perforations (arrowheads), or had a pretzel-like structure (arrows). (**D–F**) This was in striking contrast to P4 NMJs of wild-type mice, which appeared predominantly as plaques without perforations (D). For comparison, the mixture of plaques with large perforation(s) and immature pretzels that predominate at P21 and the mature pretzels that predominate in adult wild-type mice are shown in (E) and (F), respectively. (**G**) For quantification, NMJs were categorized into five distinct developmental stages, and the stage frequency patterns of the different genotypes were compared. Images show typical representatives of the distinct developmental stages of NMJs. P: Plaque; NMJs appearing as an oval or round plaque of contiguous staining for AChRs. SP: Plaque with single or multiple small perforations with a diameter of less than 1/5 of the endplate diameter. LP: Plaque with single or multiple large perforations with a diameter of more than 1/5 of the endplate diameter. Single perforations might reach the outer border of the endplate, but strip-like structures, as typical for pretzels, are not found. IP: Immature pretzel, in which strip-like structures appear. The strips of the nascent pretzels exhibit a varying width. MP: Mature pretzel, in which the strips of the pretzel exhibit a homogenous width. (**H**) Stage frequency diagram of wild-type and neurotrypsin-overexpressing mice at P4. Plaques without perforations predominate in wild-type mice. The stage distribution was shifted towards more mature stages in neurotrypsin-overexpressing mice. All characterizable endplates of four animals of each genotype were included ($n_{Wt/P4}$=1212, $n_{Tg\text{-}Nt/P4}$=458). For statistical analysis Mann-Whitney U tests were performed. (**I**) NMJ contour areas were measured separately for the different maturational stages. The average size of each maturational stage was significantly different from each other stage in both neurotrypsin-overexpressing and wild-type mice (error bars represent s.e.m., P<0.005, ANOVA with Games-Howell's post-hoc test, $n_{Tg\text{-}Nt/P4}$=10 for P, $n_{Tg\text{-}Nt/P4}$=46 for SP, n=98–106 for all other stages). The contour areas of NMJs with the same stage were identical in precociously matured NMJs of neurotrypsin-overexpressing mice at P4 and physiologically matured NMJs of wild-type mice. Scale bars: 20 µm (F) and 10 µm (G). Wt, wild-type mice; Tg-Nt, transgenic mice overexpressing neurotrypsin.

from the relatively uniform plaques found in P4 wild-type mice (Fig. 3D), but resembled in both shape and size those commonly found in wild-type mice at more advanced stages of NMJ maturation (Fig. 3E,F).

For quantification, we categorized the NMJs of wild-type and neurotrypsin-overexpressing mice at P4 into maturational stages according to Kummer and co-workers (Kummer et al., 2004). Representative images of consecutive developmental stages defined as plaque, plaque with small perforation(s), plaque with large perforation(s), immature pretzel, and mature pretzel are shown in Fig. 3G. Quantitative analysis indicated a marked shift towards mature endplates in neurotrypsin-overexpressing mice compared with wild-type mice (Fig. 3H). Immature structures, such as plaques without perforations, which predominate at P4 in wild-type mice, were virtually absent in neurotrypsin-overexpressing mice. By contrast, structures resembling immature pretzels, which are absent

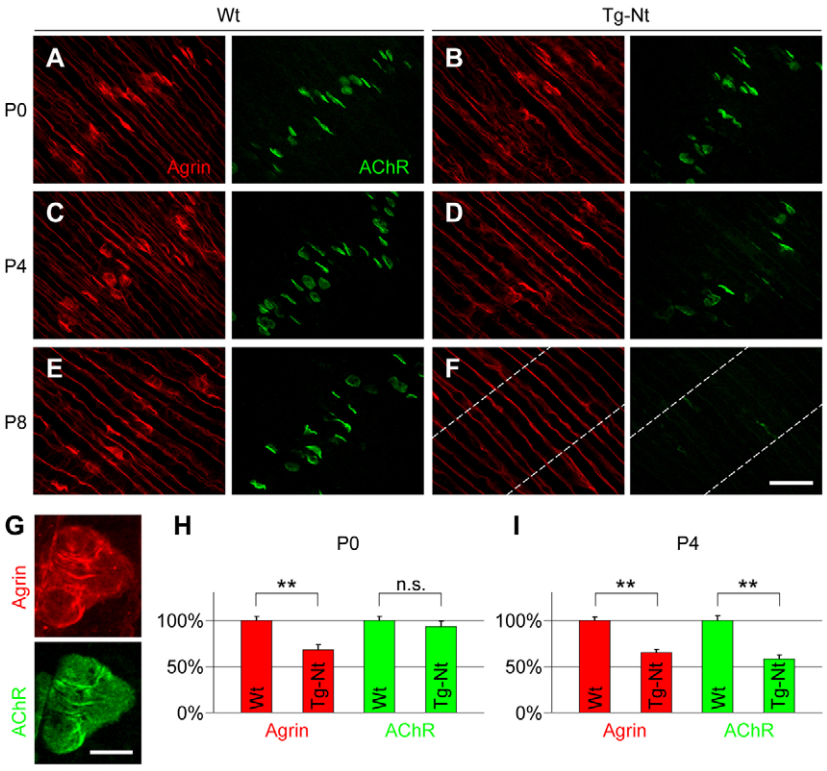

Fig. 4. Agrin reduction at the NMJ precedes reduction of AChRs and morphological features of NMJ disassembly. (**A–F**) Diaphragm NMJs from wild-type (A,C,E) and neurotrypsin-overexpressing mice (B,D,F) were double-stained for agrin (left panels, red) and AChRs (right panels, green). Images show the endplate band of diaphragm muscles. In A–E, NMJs are indicated by staining of AChRs with fluorescent α-bungarotoxin. In F, where no NMJs are seen, the region of the endplate band is indicated by white demarcation lines. After onset of neurotrypsin overexpression shortly before birth, the C-terminal part of agrin disappeared from endplates within days. Note that the neurotrypsin-dependent disappearance of endplate agrin was well matched with the disappearance of AChRs. No reduction of agrin immunoreactivity was observed on the extrasynaptic surface of the muscle fibers (D,F). (**G**) Only structures appearing as plaques or plaques with small perforations were selected for quantification, in order to include only NMJs that did not show morphological signs of precocious maturation. (**H**,**I**) Measurements of the relative fluorescence intensities for agrin and AChR in P0 (H) and P4 (I) mice indicated that neurotrypsin-dependent agrin removal from NMJs preceded the reduction in AChR density and morphological signs of NMJ disassembly. Graphs show mean ± s.e.m., $n_{Wt/P0}$=22, $n_{Tg\text{-}Nt/P0}$=21, $n_{Wt/P4}$=44, $n_{Tg\text{-}Nt/P4}$=25, two-tailed Mann-Whitney U tests; $^{**}P<0.001$; n.s., not significant. Scale bars: 50 µm (F) and 10 µm (G). Wt, wild-type mice; Tg-Nt, transgenic mice overexpressing neurotrypsin.

in wild-type mice at P4, were among the predominant shapes found in neurotrypsin-overexpressing mice. Consistent with normal NMJ growth, size measurements revealed that NMJs with advanced maturational stages were also larger in P4 neurotrypsin-overexpressing mice (Fig. 3I). Intriguingly, mature pretzels were rare and often showed fragmentation. This could indicate that the mature pretzels were relatively short-lived because of their rapid disassembly. The combination of advanced stages of developmental maturation with crumbled remnants of degenerated NMJs suggested that the neurotrypsin-overexpression phenotype found at P4 reflected a snap-shot of a precocious and dramatically accelerated plaque-to-pretzel maturation.

Reduction of agrin at NMJs precedes removal of AChRs and morphological signs of NMJ disassembly

To follow the sequence of events at NMJs after the onset of neurotrypsin overexpression in motoneurons, we investigated diaphragms during the first postnatal week (Fig. 4). Agrin immunoreactivity was monitored using a polyclonal antibody raised against the 90-kDa fragment of agrin and affinity-purified with Sepharose conjugated with pure antigen (supplementary material Fig. S5). Double-staining of NMJs for agrin and AChRs at P0 showed that agrin immunoreactivity was qualitatively identical in wild-type (Fig. 4A) and transgenic mice (Fig. 4B). In both cases, endplate agrin immunoreactivity clearly matched the α-bungarotoxin signal for AChRs (compare left and right panels of Fig. 4A,B). At P8, when the endplate band showed only very few large AChR- and synaptophysin-positive NMJs in transgenic mice, agrin-positive NMJ-like structures had also disappeared (Fig. 4F). Extrasynaptic agrin immunoreactivity was not affected by overexpression of neurotrypsin in motoneurons, indicating that loss of agrin was restricted to NMJs. At P4 in neurotrypsin-overexpressing mice (Fig. 4D), both agrin immunoreactivity and α-bungarotoxin staining showed a transition stage, characterized by a mixture of structures varying from well-conserved NMJs to small crumbled structures obviously reflecting remnants of disassembled NMJs.

To determine the onset of agrin reduction at NMJs, we analyzed double-stainings for agrin and AChRs of those endplates that were still well conserved at P4 and which closely resembled the maturational stages of endplates of age-matched wild-type mice (Fig. 4G). We considered these endplates as best suited to give insights into the early events of neurotrypsin-induced NMJ degradation, because they did not yet show any morphological features of advanced maturation, although they were destined to disassembly within days. NMJs of newborn mice, with a considerably lower level of transgenic neurotrypsin overexpression, were included for comparison. At this age, agrin but not AChR levels were already significantly reduced at NMJs of transgenic mice (Fig. 4H). At P4, when neurotrypsin overexpression was fully established, the α-bungarotoxin signal was also significantly reduced (Fig. 4I). Together, these results indicate that neurotrypsin-mediated reduction of agrin at NMJs preceded the reduction of AChR density and the first morphological signs of precocious and accelerated NMJ maturation, which in turn preceded NMJ dispersal and resumed growth of previously halted motor nerves.

Cleavage-resistant agrin rescues the neurotrypsin-overexpression phenotype at the NMJ

To study whether proteolytic cleavage of agrin is essential for the observed NMJ phenotype, we bred mouse lines with constitutive neuronal overexpression of neurotrypsin (supplementary material Fig. S6) and generated transgenic mice that overexpressed wild-type or cleavage-resistant agrin in neurons under the Thy1 promoter (supplementary material Fig. S7). Cleavage-resistant agrin was generated by exchanging the arginine and the lysine residues at the α- and β-cleavage sites of agrin, respectively, with an alanine

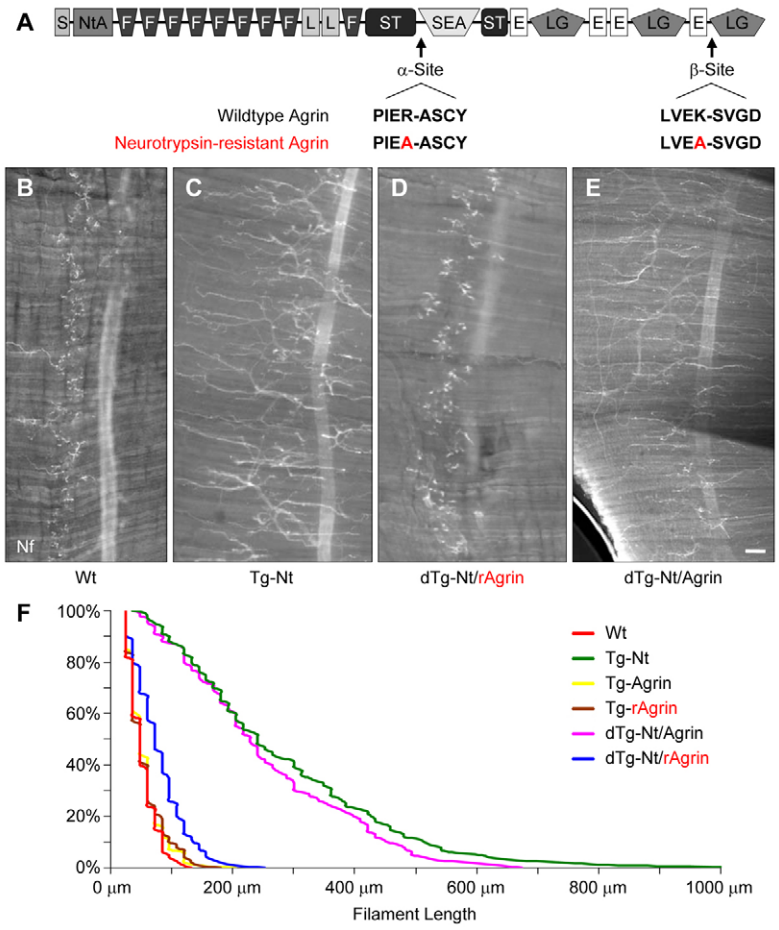

Fig. 5. Coexpression of cleavage-resistant agrin reverts the neurotrypsin-overexpression phenotype. (**A**) Domain organization and the location of the proteolytic α- and β-cleavage sites of agrin. Amino acids flanking the cleavage sites and the mutations generated to render agrin resistant to cleavage by neurotrypsin are indicated. S, signal peptide; NtA, N-terminal agrin domain; F, follistatin-like domain; L, laminin epidermal growth factor-like domain; ST, serine/threonine-rich region; SEA, sperm protein/enterokinase/agrin domain; E, epidermal growth factor-like domain; LG, laminin globular domain. (**B–E**) Representative images of the terminal nerves on the diaphragms from adult mice of different genotypes visualized with anti-neurofilament antibodies. (**F**) Quantification of axon outgrowth from the endplate band of the diaphragm in wild-type and transgenic mice. All axons emerging from the endplate band (n>190 axons per diaphragm) were measured for at least two mice of each genotype. The percentage of axons longer than a given length (y-axis) was plotted versus axon length (x-axis). The length distributions of all genotypes were statistically compared with a Kruskal-Wallis test and pairwise Mann-Whitney U tests. Axons of mice overexpressing neurotrypsin and of mice overexpressing both neurotrypsin and wild-type agrin were significantly longer than axons of all other genotypes (P<0.001). Note that co-overexpression of resistant agrin rescued from the neurotrypsin-overexpressing phenotype, whereas co-overexpression of wild-type agrin did not. Scale bar: 200 µm. Wt, wild-type mice; Tg-Nt, transgenic mice overexpressing neurotrypsin; Tg-Agrin, transgenic mice overexpressing wild-type agrin; Tg-rAgrin, transgenic mice overexpressing resistant agrin; dTg-Nt/Agrin, double-transgenic mice overexpressing neurotrypsin and wild-type agrin; dTg-Nt/rAgrin, double-transgenic mice overexpressing neurotrypsin and resistant agrin.

residue (Fig. 5A). Detailed characterizations of the individual cleavage sites had previously demonstrated that substitution of the basic P1 amino acid by alanine prevented cleavage by neurotrypsin at each site (Reif et al., 2007; Reif et al., 2008). Coexpression tests in HeLa cells confirmed the effect of these mutations by showing the resistance of double-mutated full-length agrin against proteolytic cleavage by neurotrypsin (supplementary material Fig. S8). Mice constitutively overexpressing wild-type or cleavage-resistant agrin were crossed with mice constitutively overexpressing neurotrypsin to generate double-transgenic animals. In double-transgenic mice with cleavage-resistant agrin, the motor axons ended within the endplate band (Fig. 5D), as seen in wild-type mice (Fig. 5B). Quantification of motor axon lengths confirmed the rescue effect achieved by co-overexpressing cleavage-resistant agrin in neurotrypsin-overexpressing mice (Fig. 5F). By contrast, co-overexpression of wild-type agrin together with neurotrypsin did not result in a rescue effect (Fig. 5E,F).

The reversal of the neurotrypsin-overexpression phenotype by coexpression of cleavage-resistant agrin indicates that the phenotype cannot be explained by the neurotrypsin-dependent proteolytic cleavage of other proteins and, therefore, that agrin cleavage is necessary for the phenotype. Whether agrin cleavage is sufficient for the phenotype cannot be determined without testing for a contribution of all proteins of the NMJ. This is obviously not possible. However, we did test several NMJ components with an established role in NMJ development and maintenance for susceptibility of proteolytic cleavage by neurotrypsin, including the agrin receptor lipoprotein receptor-like protein 4 (LRP4) and its co-receptor muscle-specific kinase (MuSK), the agrin ligands dystroglycan and laminin, as well as the neuregulin receptors ErbB2, ErbB3 and ErbB4. As shown in supplementary material Fig. S9, none of these proteins was cleaved by neurotrypsin. These results corroborated previous indications of a highly selective proteolytic activity of neurotrypsin versus agrin (Reif et al., 2007; Reif et al., 2008).

NMJ maturation is delayed in double-transgenic mice overexpressing neurotrypsin and cleavage-resistant agrin, but not in neurotrypsin-deficient mice

Because excessive agrin cleavage by neurotrypsin enhanced NMJ maturation, we wondered whether reduced agrin cleavage would result in delayed NMJ maturation. To this end, we studied NMJ maturation from the initial oval plaque to the mature pretzel form in diaphragms of mice exhibiting distinct levels of agrin cleavage. We found that NMJ maturation in mice overexpressing cleavage-resistant agrin together with neurotrypsin was considerably delayed. At P42, when 90% of the NMJs of wild-type mice had reached the mature pretzel stage (Fig. 6A), double-transgenic mice overexpressing both neurotrypsin and cleavage-resistant agrin had endplates with perforations, but no mature pretzels (Fig. 6B).

For quantification, stages of plaque-to-pretzel development were determined according to Kummer and co-workers (Kummer et al., 2004). Representative images of the consecutive developmental stages are shown in Fig. 3G. We staged NMJs in the endplate band of the diaphragm at P9, P21, P42 and P90, because normal NMJ maturation in this muscle takes approximately 5–6 weeks. We found that the marked delay in

NMJ maturation in mice overexpressing neurotrypsin together with cleavage-resistant agrin was also evident at P21. At this age, most NMJs of wild-type mice had developed to plaques with large perforations and immature pretzels, whereas only a minority of the NMJs of double-transgenic mice had developed beyond the initial plaque stage (Fig. 6H). Analysis at P90 showed that only approximately 60% of the endplates had reached the mature pretzel stage (Fig. 6J). No difference to wild-type mice was found at P9 (Fig. 6G). These results indicated that coexpression of cleavage-resistant agrin together with neurotrypsin inhibited the structural transformation of the NMJs and, thus, delayed plaque-to-pretzel maturation.

By contrast, NMJs of mice overexpressing neurotrypsin and wild-type agrin were indistinguishable from those of mice overexpressing neurotrypsin alone when analyzed at P21, P42 and P90. At these ages, only crumbled residual fragments of endplates were found. Plaques or pretzels with a morphology that was appropriate for inclusion in one of the defined maturation stages could only be identified at P9 (Fig. 6G). At this age, approximately 50% of the endplates were 'stageable'. Their distribution pattern showed an increased proportion of advanced plaque stages, indicating accelerated maturation as compared with wild-type mice. Because stageable endplates were last seen at P4 in mice overexpressing neurotrypsin alone, our results found in mice overexpressing both neurotrypsin and wild-type agrin at P9 indicate that the higher levels of agrin slowed down, but did not prevent, the accelerated passage through the structural transformation found in the presence of excessive levels of neurotrypsin alone. Endplates of mice overexpressing agrin in wild-type or cleavage-resistant form alone were indistinguishable from those of wild-type mice (Fig. 6D,E,G–J).

Neurotrypsin-deficient mice, which do not show any indication of agrin cleavage in the brain (Matsumoto-Miyai et al., 2009; Reif et al., 2007; Stephan et al., 2008) and the spinal cord (supplementary material Fig. S10), showed normal endplate maturation (Fig. 6F–J). At P42, normal pretzel structures were predominant, as in wild-type mice, indicating a timely conclusion of the maturation process (Fig. 6F,I). Quantification of the distinct maturation stages from P9 through P90 showed the same distribution patterns as found for wild-type mice.

Together, our results clearly demonstrate a delayed NMJ maturation when cleavage-resistant agrin is coexpressed with overexpressed neurotrypsin, but normal maturation in the absence of neurotrypsin.

Discussion

Transgenic upregulation of neurotrypsin in motoneurons results in reduced amounts of agrin at NMJs and is followed by NMJ disassembly

We found that overexpression of neurotrypsin in motoneurons produced a phenotype that resembled the 'agrin/LRP4/MuSK/rapsyn-deficiency' phenotype of the diaphragm muscle (DeChiara et al., 1996; Gautam et al., 1995; Gautam et al., 1996; Weatherbee et al., 2006). Motor axons did not end in presynaptic terminals within the central endplate band, but grew diffusely over the muscle. Immature presynaptic structures, characteristically appearing as en passant or terminal varicosities of motor axons with clusters of enclosed synaptic vesicles, were found all over the muscle surface. Terminal arborizations were rarely seen. On the postsynaptic side, neurotrypsin overexpression closely resembled the phenotype of agrin-deficient mice, but was distinct from the MuSK- and rapsyn-deficiency phenotypes. Whereas muscles of MuSK- and rapsyn-deficient mice typically did not exhibit any AChR clusters at all, both neurotrypsin-overexpressing and agrin-deficient mice did have weakly stained AChR clusters. We concluded that the NMJ phenotype of neurotrypsin-overexpressing mice was compatible with a role of neurotrypsin as an inactivator of agrin function at the NMJ.

Constitutive inactivation of agrin, LRP4, MuSK or rapsyn by gene targeting is lethal at birth due to a severe defect in NMJ formation (DeChiara et al., 1996; Gautam et al., 1995; Gautam et al., 1996; Weatherbee et al., 2006). By contrast, the phenotype induced by neurotrypsin overexpression in motoneurons is compatible with life. Probably, Cre-mediated activation of the transgene results in a variable extent of neurotrypsin overexpression in different motoneurons. Lesser agrin cleavage in some motoneurons with lower levels of transgenic neurotrypsin might be sufficient to preserve corresponding NMJs. Indeed, in rare cases large synapses with mature postsynaptic folding were found within the endplate band. Moreover, many ectopic NMJs in adult neurotrypsin-overexpressing mice were not completely devoid of postsynaptic folds, but had a small number of short invaginations (Fig. 1K), indicating that partial maturation could have occurred in some of the ectopic NMJs.

In contrast to the targeted inactivation of the agrin gene, the experimental upregulation of neurotrypsin established the 'agrin-deficiency' phenotype postnatally after NMJs had already been formed. At birth, when overexpression of neurotrypsin was induced but still low, a reduction of NMJ agrin could be measured, although no morphological features of the later phenotype were apparent. At P4, with the full transgenic upregulation of neurotrypsin established, the number of NMJs within the endplate band was markedly reduced. Motor nerves of dissolved NMJs had started to grow out of the endplate band, but only few ectopic synapses were found. At P8, dissolution of the previously established NMJs of the endplate band was virtually completed. Our results demonstrate a delay of a few days between the maximal upregulation of neurotrypsin and the establishment of the full NMJ phenotype. The detailed temporal analysis of transgene expression indicated that NMJ disassembly was preceded by reduction of NMJ agrin. Together, these observations point to a chain of events that starts with the upregulation of neurotrypsin in motoneurons, resulting in turn in enhanced cleavage of agrin in motoneurons or at the NMJ and, thus, a reduced endowment of the NMJ with agrin in its full-length, synapse-protecting form. As a result, the NMJ is disassembled within days. These results strongly support a role of agrin as a synapse-protecting factor against a nerve-dependent, muscle-resident dispersal mechanism (Kummer et al., 2006).

The site of agrin cleavage attributable to transgenic upregulation of neurotrypsin in motoneurons cannot be definitively determined on the basis of our results. Agrin might be cleaved in motoneurons upon its intracellular encounter with transgenic neurotrypsin. Alternatively, agrin cleavage might occur at the NMJ, when axonally transported neurotrypsin encounters previously deposited agrin. We favor the idea that transgenic neurotrypsin cleaves agrin within motoneurons, e.g. in the Golgi complex or along the axonal secretory pathway, because we were unable to locate neurotrypsin at the NMJ, despite numerous experimental attempts. However, cleavage at both locations might affect the NMJs in the same way, because in both cases a reduced endowment of the NMJs with full-length, synapse-protecting agrin might result.

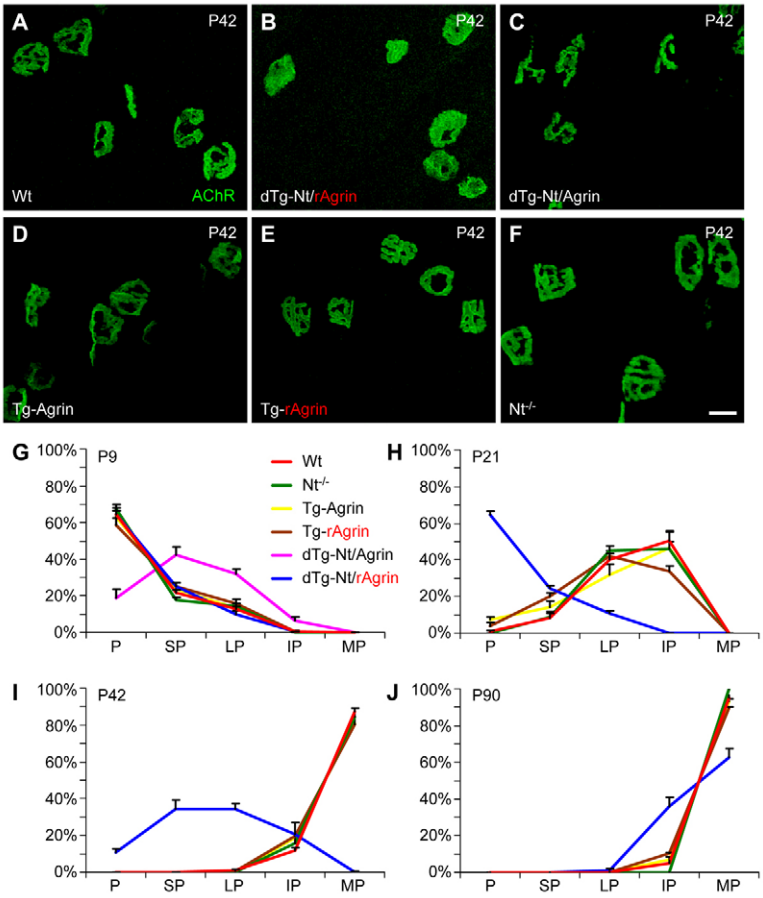

Fig. 6. Stage frequency patterns indicate cleavage-resistant agrin and, to a lesser degree, wild-type agrin as delaying factors for plaque-to-pretzel maturation. NMJs of the diaphragms from mice of different genotypes were stained at P9, P21, P42 and P90 with fluorescent α-bungarotoxin, and the maturational states in different genotypes were compared. (**A**) NMJs of P42 wild-type mice had matured, and most had reached one of the pretzel stages. (**B**) NMJs of mice co-overexpressing neurotrypsin together with cleavage-resistant agrin appeared as plaques with no or only small perforations. They resembled NMJs of wild-type mice at P4. (**C**) Muscles of mice co-overexpressing neurotrypsin together with wild-type agrin had lost most of their NMJs. The remaining NMJ structures could not be categorized. They resembled NMJ remnants of single transgenic animals overexpressing neurotrypsin. (**D**–**F**) NMJs of mice overexpressing either wild-type agrin (D) or cleavage-resistant agrin (E), or of neurotrypsin-deficient mice (F) did not differ from those of wild-type mice (A). NMJs were categorized into five distinct developmental stages, as indicated in Fig. 3G. (**G**) At P9, plaques without perforations predominate in wild-type mice and all other strains, except double-transgenic mice overexpressing neurotrypsin together with wild-type agrin. In these animals, NMJs differed significantly from all other genotypes, because their stage distribution was shifted towards more mature stages. (**H**) At P21, perforated plaques and immature pretzels predominated in wild-type mice. The stage frequency distribution of double-transgenic mice overexpressing neurotrypsin together with cleavage-resistant agrin differed significantly from that of wild-type mice and all other genotypes (P<0.001). Their stage distribution was shifted towards immature stages. (**I**) At P42, over 85% of the NMJs of wild-type mice had reached the mature pretzel stage. Development of NMJs of double-transgenic mice overexpressing neurotrypsin together with cleavage-resistant agrin was markedly delayed. They populated predominantly the perforated plaque stages. Only approximately 20% of the NMJs had developed into immature pretzels. (**J**) At P90, almost all NMJs of wild-type mice had developed into mature pretzels. NMJs of double-transgenic mice overexpressing neurotrypsin together with cleavage-resistant agrin still exhibited a considerable retardation, because 35% exhibited clear characteristics of immature pretzels. All characterizable endplates of at least three animals of each genotype on P9, P21, P42 and P90 were included ($n_{Nt^{-/-}/P21}$=318, $n_{Tg\text{-}Agrin/P42}$=282, $n_{Wt/P90}$=413, n>500 for all others). For statistical analysis, a Kruskal-Wallis test and pairwise Mann-Whitney U tests were performed. Note: NMJs of single-transgenic neurotrypsin-overexpressing mice could not be included at time points later than P4 (Fig. 3), because only crumbled remnants that could not be categorized were found in older mice. NMJs of double-transgenic mice overexpressing neurotrypsin together with wild-type agrin could only be staged at P9, because only crumbled remnants but no 'stageable' endplates were found at later time points. Scale bar: 20 µm. Wt, wild-type mice; $Nt^{-/-}$, neurotrypsin-deficient mice; Tg-Agrin, transgenic mice overexpressing wild-type agrin; Tg-rAgrin, transgenic mice overexpressing resistant agrin; dTg-Nt/Agrin, double-transgenic mice overexpressing neurotrypsin and wild-type agrin; dTg-Nt/rAgrin, double-transgenic mice overexpressing neurotrypsin and resistant agrin; P, plaque; SP, plaque with small perforation(s); LP, plaque with large perforation(s); IP, immature pretzel; MP, mature pretzel.

Agrin cleavage as a regulator of NMJ maturation

The process of NMJ maturation from the oval plaque, which is found in rodents at birth, to the mature pretzel-like structure is characterized by reorganizations on both the pre- and postsynaptic sides, including the removal of receptors and other components of the postsynaptic specialization (Desaki and Uehara, 1987; Marques et al., 2000; Sanes and Lichtman, 2001; Slater, 1982). We found that the progress of plaque-to-pretzel maturation was dramatically enhanced by overexpression of neurotrypsin in motoneurons, with precocious and accelerated NMJ maturation ending in disassembly of the synapse within days. Instead of a maturation period of 4–6 weeks, as found for NMJs in wild-type mice, endplates of

neurotrypsin-overexpressing mice required only a few days to reach the pretzel stage. The highly similar NMJ morphologies found during developmental plaque-to-pretzel maturation and during NMJ disassembly induced by neurotrypsin overexpression in motoneurons suggest a common underlying mechanism. The excessively activated 'maturational' processes with a highly accelerated passage through the plaque-to-pretzel stages in neurotrypsin-transgenic mice is consistent with reduced NMJ stabilization due to reduced levels of full-length agrin at the NMJs of these mice.

Intriguingly, coexpression of cleavage-resistant agrin not only simply rescued the phenotype of neurotrypsin overexpression, but established its own phenotype by delaying plaque-to-pretzel maturation of the NMJs. Because NMJ maturation proceeded at normal speed in neurotrypsin-deficient mice, the maturational delay phenotype of resistant agrin cannot be explained simply as substrate-dependent blockade of neurotrypsin-dependent agrin cleavage. Rather, the presence of cleavage-resistant agrin at the NMJ must directly interfere with the maturation process. This is supported by our finding that NMJ maturation in mice overexpressing agrin alone, either the wild-type or the cleavage-resistant form, was indistinguishable from NMJ maturation in wild-type mice (Fig. 6). Maturation was delayed only when cleavage-resistant agrin was coexpressed with excessive neurotrypsin that reduced levels of cleavable agrin at the NMJ (Figs 4, 6). These results suggest that NMJ maturation requires local agrin turnover. Replacement of cleavable agrin with the cleavage-resistant form results in a slow-down of the maturational process, because the pool of cleavable agrin becomes gradually smaller. By contrast, delivery of cleavage-resistant agrin to already 'saturated' NMJs at birth (due to the use of the Thy-1 promoter) in single transgenic mice might not allow for its efficient deposition and replacement of wild-type agrin. Therefore, we speculate that the NMJ maturation-delaying effect of cleavage-resistant agrin occurs as a result of its deposition at the NMJ.

A protease distinct from neurotrypsin must cleave agrin at the NMJ

In wild-type mice, agrin cleavage at the NMJ must be independent of neurotrypsin, because NMJ maturation was normal in neurotrypsin-deficient mice (Fig. 6). The presumed protease responsible for selective cleavage of agrin at the NMJ remains to be identified. This protease should not be expressed in the CNS, because our screens for agrin fragments indicated that agrin was not cleaved in the brain (Matsumoto-Miyai et al., 2009; Reif et al., 2007; Stephan et al., 2008) and spinal cord (supplementary material Fig. S10) of neurotrypsin-deficient mice. The enzymatic characteristics of the postulated protease should be very similar to neurotrypsin, because its proteolytic function should also depend on the presence of the P1 basic residue at each cleavage site of agrin (Reif et al., 2007; Reif et al., 2008). An isoenzyme of neurotrypsin with a different expression pattern can be excluded, because only one neurotrypsin gene is found in the murine genome. Moreover, screening for trypsin-like serine proteases with a similar cleavage site preference has not revealed any candidates.

A plausible candidate for an agent relieving the constraint of agrin on NMJ maturation would be matrix metalloproteinase-3 (MMP-3). MMP-3 is located at the NMJ and has been reported to cleave agrin at the NMJ in an activity-dependent manner (Werle and VanSaun, 2003). However, the MMP-3-dependent cleavage of agrin was localized within the sequence PHT-MLNLKE in the second laminin G domain (VanSaun et al., 2003). Therefore, it is unlikely that the arginine-to-alanine and the lysine-to-alanine point mutations that we introduced at the distant α- and β-cleavage sites would have rendered agrin resistant to MMP-3. Still, we assessed plaque-to-pretzel maturation in MMP-3-deficient mice and found that it proceeded at the same rate as in wild-type mice (data not shown). Because plasminogen was suggested to be an activator of Pro-MMP-3 (VanSaun and Werle, 2000), we also tested plaque-to-pretzel maturation in plasminogen-deficient mice. Again, we found no difference to wild-type mice (data not shown). These results exclude MMP-3 as a candidate for the postulated local agrin-cleaving protease at the NMJ.

Conclusion

Our results suggest that the agrin-dependent stabilization of the NMJ represents a constraint on the reorganization underlying NMJ maturation. To allow plaque-to-pretzel maturation of the NMJ to proceed, the agrin-dependent constraint needs to be relieved by proteolytic cleavage of agrin. We propose that the phenotypes observed in the absence of or with excessive cleavage of agrin represent the extreme activity states of a reorganizational process that removes receptors and other postsynaptic components from the NMJ to serve the developmental sculpting of the NMJ from its initial oval plaque to the mature pretzel-like structure. The molecular and cellular nature of the reorganization process during NMJ maturation is currently not known. Observations with cultured myotubes indicated that plaque-to-pretzel maturation can occur without neural input and, therefore, in the absence of neural agrin (Kummer et al., 2004). These results suggest that relief of the agrin-mediated stabilization in vivo could suffice to allow NMJs to mature.

Materials and Methods

Mouse strains

All animal procedures were executed in accordance with institutional guidelines for animal care and were approved by the Veterinary Authority of the Canton Zurich.

Neurotrypsin-deficient mice

The generation of neurotrypsin-deficient mice lacking the protease domain, and western blots showing absence of agrin cleavage in their brains, were reported previously (Matsumoto-Miyai et al., 2009; Reif et al., 2007; Stephan et al., 2008).

Transgenic mice for conditional overexpression of neurotrypsin

Neurotrypsin was overexpressed under the control of the promoter of the Thy1.2 allele of the Thy1 gene (Gordon et al., 1987; Caroni, 1997). Because constitutive overexpression of neurotrypsin under this promoter was perinatally lethal (supplementary material Fig. S1), we generated transgenic mice bearing a dormant (conditional) transgene by insertion of a transcriptional stop signal flanked by *loxP* sites between the Thy1 promoter and the neurotrypsin-encoding segment (supplementary material Fig. S2). The transcriptional stop cassette consisted of a 1.3-kbp-long segment of the pBS302 plasmid (Invitrogen), containing a false translational start codon (ATG), a splice donor signal, and an SV40 polyadenylation signal (Lakso et al., 1992; Sauer, 1998). To generate the pThy1-*loxP*-Stop-*loxP*-Nt construct a *Xho*I fragment containing the human neurotrypsin cDNA was ligated into the *Msc*I site of pBS302, and a *Xho*I-*Bam*HI fragment was ligated into the *Eco*RI site of pBS302. For murine neurotrypsin, a *Nar*I-*Pvu*I fragment containing the cDNA was inserted into the *Msc*I site of pBS302, and a *Hin*dIII-*Eco*RV fragment was inserted into the *Eco*RI site of pBS302. The fragments containing the floxed stop cassette in either orientation followed by the neurotrypsin cDNA were excised with *Not*I and inserted into the *Xho*I site of the murine Thy1.2 expression cassette (Caroni, 1997). The transgenic insert was isolated from the vector with *Pvu*I and injected into fertilized mouse oocytes according to standard protocols (Rulicke, 2004). The litters were genotyped by PCR with a 5′-primer corresponding to a sequence inside the neurotrypsin cDNA (5′-GCAATGTGCCAGATTCAGCAG-3′ for human neurotrypsin and 5′-CAATGTGCCAGACTAAGCACC-3′ for murine neurotrypsin) and a 3′-primer corresponding to a sequence inside the Thy1.2 expression cassette downstream of the insertion site of the neurotrypsin cDNA (5′-CCCATGTTCTGAGATATTGGAAG-3′). We found that the *loxP*-Stop-*loxP* cassette completely suppressed transgene expression (supplementary material Fig. S2) and abolished the lethal phenotype observed with constitutive transgene expression, not

only when it was inserted as initially described (Lakso et al., 1992; Sauer, 1998), but also in the inverted orientation.

Transgenic mice with selective overexpression of neurotrypsin in spinal cord motoneurons

Mice bearing the conditional constructs (lines 497, 498 and 533 for murine neurotrypsin, and lines 491, 493 and 494 for human neurotrypsin) were crossed with mice expressing Cre recombinase under the control of the motoneuron-specific Hb9 promoter (Yang et al., 2001) to induce recombination between *loxP* sites and selective activation of the pThy1-Nt transgene in motoneurons (supplementary material Fig. S3). The litters were genotyped by PCR. The presence of transgenic neurotrypsin was tested as specified above. The presence of Cre recombinase was tested with the primers 5′-GGAAAATAGCGATCGCTGC-3′ and 5′-CACCAGCTTGCATG-ATCTCC-3′. We found that all transgenic animals derived via Cre recombinase-mediated excision from conditional transgenic mice bearing a *loxP*-Stop-*loxP* cassette were viable. The expression of the transgene was verified at the protein level by western blotting (supplementary material Fig. S3). The proteolytic activity of transgenic neurotrypsin was assessed by western blotting of the 90-kDa fragment of agrin, which results from cleavage at both the α- and the β-site (supplementary material Fig. S4). Various expression levels were found in both types of constructs after Cre recombinase-mediated excision of the transcriptional stop segment.

Transgenic mice with constitutive overexpression of neurotrypsin

To generate mouse lines with constitutive overexpression of neurotrypsin we crossed conditional transgenic mice of line B6.C3-*Tg*(PRSS12) 491 Zbz with transgenic mice expressing Cre recombinase under the control of the cytomegalovirus (CMV) promoter, resulting in early *loxP*-based recombination and the germline transmission of the excised state (supplementary material Fig. S6). Expression and proteolytic activity of transgenic neurotrypsin were assessed by western blotting (supplementary material Fig. S6). We found an increase of agrin-90 in spinal cord homogenates.

Transgenic mice overexpressing inactive neurotrypsin

Inactive neurotrypsin (iNt) was generated by mutating the essential active site serine 711 (corresponding to serine 195 of chymotrypsin) to alanine (supplementary material Fig. S1). To generate the pThy1-iNt construct a PCR fragment was amplified using a mouse neurotrypsin cDNA as template and 5′-CGTGTGGACAGCTGCC-AGGGAGACGCTGGAGGA-3′ and 5′-CTCAAGCTTAGTTACAGACTGGT-GACACTTTTTATC-3′ as primers. This fragment was reintroduced into the vector containing a full-length neurotrypsin cDNA. The mutated cDNA was then excised and subcloned into the *Xho*I site of the Thy1.2 cassette. The construct was linearized and injected into the pronuclei of fertilized mouse oocytes. Litters were screened by PCR on genomic DNA using the primers 5′-CCCATCCACATGGATAATGT-GAA-3′ and 5′-CCCATGTTCTGAGATATTGGAAG-3′. Mice overexpressing inactive neurotrypsin under the Thy1 promoter were viable and did not express any abnormalities. Overexpression of neurotrypsin and levels of agrin-90 in this line are shown in supplementary material Fig. S4. Quantification indicated that agrin-90 was at wild-type levels.

Transgenic mice overexpressing agrin

Wild-type or cleavage-resistant agrin (mutation of the α-cleavage site arginine to lysine and the β-cleavage site lysine to alanine to render it resistant to neurotrypsin cleavage; supplementary material Fig. S8) were overexpressed under the Thy1 promoter (supplementary material Fig. S7). To generate the transgenic construct, the cDNA of the transmembrane form of rat agrin (NCBI reference sequence: NM_175754) was subcloned into pBluescript. Arginine 995 of the α-cleavage site and lysine 1754 of the β-cleavage site (NCBI reference sequence: NP_786930) were both mutated to alanine by site-directed PCR mutagenesis and thereby rendered resistant to neurotrypsin cleavage, as demonstrated in supplementary material Fig. S8. The 5′ end of the secreted form of agrin up to the first follistatin domain was obtained by RT-PCR using primers 5′-CGCATCGATGTTCCGGGCTGCGC-CATGGTCC-3′ and 5′-GTCCCGGGACCCACATGGCCCTTG-3′, and total RNA from mouse spinal cord as template. The 5′ region of transmembrane rat agrin upstream of the *Sma*I restriction site immediately following the DNA region encoding the first follistatin domain was then replaced by the 5′ region of secreted murine agrin. The assembled DNA sequences of mutant (cleavage-resistant) and wild-type agrin were inserted into the Thy1.2 expression cassette. The DNA fragments were injected into the pronuclei of fertilized oocytes. The transgenic overexpression of agrin in neurons was confirmed by immunocytochemical staining (supplementary material Fig. S7).

Double-transgenic mice overexpressing neurotrypsin and agrin

To overexpress neurotrypsin in combination with agrin, the constitutive neurotrypsin-overexpressing line B6.C3-*Tg*(PRSS12) 491.1 Zbz was crossed with mice of lines B6;D2-*Tg*(Agrn) 1380, 1381 Zbz (for wild-type agrin) or mice of lines B6;D2-*Tg*(Agrn$^{(R995A;K1754A)}$) 1385, 1386 Zbz (for cleavage-resistant agrin).

Antibodies

The rabbit antiserum SZ177 was generated against two synthetic peptides corresponding to amino acids 22–40 and 45–57 of mouse neurotrypsin. The goat antiserum G87 was raised against the protease domain of human neurotrypsin (produced in *Escherichia coli*) and affinity-purified. The goat antiserum G93 was generated against full-length mouse neurotrypsin (produced in stably transfected mouse myeloma J558L cells). The rabbit antiserum R132 was raised against the 90-kDa fragment of rat agrin (produced in HEK293T cells) and affinity-purified. The rabbit antiserum R139 was generated against purified recombinant agrin-22. Rabbit anti-neurofilament antibodies were purchased from Chemicon, mouse anti-neurofilament (clone NR4) and rabbit anti-synaptophysin from DakoCytomation, and mouse anti-β-actin (clone AC-74) from Sigma. Secondary antibodies for immunoblotting (peroxidase conjugates) were from Sigma and KPL. Secondary antibodies for immunofluorescence (Cy2, Cy3, Cy5 or Rhodamine Red-X conjugates) were from Jackson ImmunoResearch.

Electrophoresis and immunoblotting

From spinal cord extracts

Spinal cord extracts were prepared by lysing the tissues in extraction buffer (150 mM NaCl, 1% Triton X-100, protease inhibitors, in 20 mM Tris-HCl, pH 7.5). After homogenization and centrifugation of the extracts, supernatants were collected and protein concentrations were measured by a Bradford assay (Bio-Rad Laboratories). Proteins were resolved by SDS-PAGE on 8% gels and blotted to PVDF membranes (Millipore). Immunological detection was performed as described previously (Stephan et al., 2008).

From transfected cell lines

The day before transfection cells (HEK293T or HeLa) were seeded in six-well plates in 2 ml DMEM supplemented with 10% FCS. Before transfection, the medium was removed, cells were washed with PBS, and DMEM was added. For transfection, we used the calcium phosphate precipitation method or Lipofectamine 2000 (Invitrogen) with a total of 5 μg plasmid DNA. In double transfection experiments, 2.5 μg of each plasmid were co-transfected. In single transfection experiments, 2.5 μg of a specific cDNA was co-transfected with 2.5 μg of empty pcDNA3.1 vector to reach 5 μg. To test laminin for cleavage by neurotrypsin, HEK293EBNA cells stably expressing laminin-2 (laminin-211) (Aumailley et al., 2005) were transfected with 2.5 μg neurotrypsin cDNA and 2.5 μg empty pcDNA3.1 vector using the polyethylenimine transfection method. At 24–48 hours after transfection, the supernatant was collected and the cells lysed with 20 mM Tris-HCl, pH 7.5, containing 150 mM NaCl, 0.5 mM EDTA, and 1% Triton X-100. Cell lysate (10 μl) was subjected to SDS-PAGE and subsequently electrotransferred to PVDF or nitrocellulose membranes.

Immunostainings

Diaphragms

Diaphragms were dissected, rinsed in PBS, and fixed in methanol at –20°C for 10 minutes. After washing in PBS, the muscles were incubated in blocking solution (5% horse serum, 1% BSA, 1% Triton X-100, 0.1% sodium azide, in PBS) for 2 hours, followed by incubation with primary antibodies in blocking solution overnight at 4°C. After washing in PBS containing 0.5% Triton X-100, muscles were incubated with secondary antibodies and Alexa Fluor 488-conjugated α-bungarotoxin (10 nM; Molecular Probes) for 4 hours. After washing, samples were embedded in DAKO mounting medium. Z-serial images were collected using a Leica SP1 confocal laser scanning microscope. To quantitate agrin and α-bungarotoxin signals, endplates from wild-type and neurotrypsin-overexpressing mice were imaged with identical microscope and detector settings (100× objective). Only endplates located on top of fibers at the surface of the muscle were included in the analysis. Using the Leica confocal software, an elliptical region of interest of 10 μm^2 area was set within an endplate, and the maximum amplitudes were determined from the fluorescence stack profiles of both channels (three measurements per endplate).

Spinal cords

Spinal cords from 3-month-old mice were dissected, embedded in Tissue-Tek (Sakura Finetek), and frozen in isopentane at –70°C. Consecutive 12-μm thick cross-sections were cut on a Leica cryostat, mounted on glass slides and air-dried. The sections were fixed in 4% paraformaldehyde in PBS and washed in PBS. Consecutive sections were stained with antibodies against agrin and with cresyl violet to identify the motoneurons. For immunostaining the sections were blocked for 2 hours in blocking solution (5% horse serum, 1% BSA, 1% Triton X-100, in PBS), followed by incubation with primary antibodies against agrin (R132, affinity purified, 1.1 μg/ml) or with preimmune Ig (2.0 μg/ml) in blocking solution for 16 hours at 4°C. After washing in PBS containing 0.5% Triton X-100, the sections were incubated with Cy3-conjugated secondary antibodies for 4 hours.

Electron microscopy

Diaphragms were excised and fixed with 2% glutaraldehyde in 100 mM cacodylate buffer, pH 7.4, overnight at 4°C. After several washes in the same buffer, small pieces of the nerve/muscle contact area were dissected, postfixed with 1% osmium tetroxide in cacodylate buffer, dehydrated, and embedded in epoxy resin (Epon 812). Thin sections were cut on a Reichert ultracut E ultramicrotome, stained with uranyl acetate and lead citrate, and examined with a Philips CM10 transmission electron microscope.

We thank Daniel Blaser, Monica Dilkin, and Virginia Meskenaite for mouse husbandry, Silvia Arber and Thomas M. Jessell for the pHb9-Cre mouse line, Joshua R. Sanes for agrin-deficient mice, Jean-Marie Stassen for plasminogen-deficient mice, Karl W. K. Tsim for the agrin cDNA, Lin Mei for the LRP4 cDNA, Steven J. Burden for the MuSK cDNA, and John G. Koland for the ErbB4 cDNA. The dystroglycan cDNA was obtained from RZPD Deutsches Ressourcenzentrum für Genomforschung. A stable HEK293EBNA cell line expressing laminin-2 was provided by Peter D. Yurchenco. This work was supported by the Swiss National Science Foundation, the Novartis Foundation, the Betty and David Koetser Foundation, the Olga Mayenfisch Foundation, the Helmut Horten Foundation, and the Hartmann Müller Foundation.

Supplementary material available online at
http://jcs.biologists.org/cgi/content/full/123/22/3944/DC1

References

Arber, S., Han, B., Mendelsohn, M., Smith, M., Jessell, T. M. and Sockanathan, S. (1999). Requirement for the homeobox gene Hb9 in the consolidation of motor neuron identity. *Neuron* **23**, 659-674.

Aumailley, M., Bruckner-Tuderman, L., Carter, W. G., Deutzmann, R., Edgar, D., Ekblom, P., Engel, J., Engvall, E., Hohenester, E., Jones, J. C. et al. (2005). A simplified laminin nomenclature. *Matrix Biol.* **24**, 326-332.

Bezakova, G. and Ruegg, M. A. (2003). New insights into the roles of agrin. *Nat. Rev. Mol. Cell Biol.* **4**, 295-308.

Caroni, P. (1997). Overexpression of growth-associated proteins in the neurons of adult transgenic mice. *J. Neurosci. Methods* **71**, 3-9.

DeChiara, T. M., Bowen, D. C., Valenzuela, D. M., Simmons, M. V., Poueymirou, W. T., Thomas, S., Kinetz, E., Compton, D. L., Rojas, E., Park, J. S. et al. (1996). The receptor tyrosine kinase MuSK is required for neuromuscular junction formation in vivo. *Cell* **85**, 501-512.

Desaki, J. and Uehara, Y. (1987). Formation and maturation of subneural apparatuses at neuromuscular junctions in postnatal rats: a scanning and transmission electron microscopical study. *Dev. Biol.* **119**, 390-401.

Gautam, M., Noakes, P. G., Mudd, J., Nichol, M., Chu, G. C., Sanes, J. R. and Merlie, J. P. (1995). Failure of postsynaptic specialization to develop at neuromuscular junctions of rapsyn-deficient mice. *Nature* **377**, 232-236.

Gautam, M., Noakes, P. G., Moscoso, L., Rupp, F., Scheller, R. H., Merlie, J. P. and Sanes, J. R. (1996). Defective neuromuscular synaptogenesis in agrin-deficient mutant mice. *Cell* **85**, 525-535.

Gordon, J. W., Chesa, P. G., Nishimura, H., Rettig, W. J., Maccari, J. E., Endo, T., Seravalli, E., Seki, T. and Silver, J. (1987). Regulation of Thy-1 gene expression in transgenic mice. *Cell* **50**, 445-452.

Kummer, T. T., Misgeld, T., Lichtman, J. W. and Sanes, J. R. (2004). Nerve-independent formation of a topologically complex postsynaptic apparatus. *J. Cell Biol.* **164**, 1077-1087.

Kummer, T. T., Misgeld, T. and Sanes, J. R. (2006). Assembly of the postsynaptic membrane at the neuromuscular junction: paradigm lost. *Curr. Opin. Neurobiol.* **16**, 74-82.

Lakso, M., Sauer, B., Mosinger, B., Jr, Lee, E. J., Manning, R. W., Yu, S. H., Mulder, K. L. and Westphal, H. (1992). Targeted oncogene activation by site-specific recombination in transgenic mice. *Proc. Natl. Acad. Sci. USA* **89**, 6232-6236.

Lin, S., Landmann, L., Ruegg, M. A. and Brenner, H. R. (2008). The role of nerve- versus muscle-derived factors in mammalian neuromuscular junction formation. *J. Neurosci.* **28**, 3333-3340.

Marques, M. J., Conchello, J. A. and Lichtman, J. W. (2000). From plaque to pretzel: fold formation and acetylcholine receptor loss at the developing neuromuscular junction. *J. Neurosci.* **20**, 3663-3675.

Matsumoto-Miyai, K., Sokolowska, E., Zurlinden, A., Gee, C. E., Luscher, D., Hettwer, S., Wolfel, J., Ladner, A. P., Ster, J., Gerber, U. et al. (2009). Coincident pre- and postsynaptic activation induces dendritic filopodia via neurotrypsin-dependent agrin cleavage. *Cell* **136**, 1161-1171.

McMahan, U. J. (1990). The agrin hypothesis. *Cold Spring Harbor Symp. Quant. Biol.* **55**, 407-418.

Nguyen, Q. T., Son, Y. J., Sanes, J. R. and Lichtman, J. W. (2000). Nerve terminals form but fail to mature when postsynaptic differentiation is blocked: in vivo analysis using mammalian nerve-muscle chimeras. *J. Neurosci.* **20**, 6077-6086.

Reif, R., Sales, S., Hettwer, S., Dreier, B., Gisler, C., Wolfel, J., Luscher, D., Zurlinden, A., Stephan, A., Ahmed, S. et al. (2007). Specific cleavage of agrin by neurotrypsin, a synaptic protease linked to mental retardation. *FASEB J.* **21**, 3468-3478.

Reif, R., Sales, S., Dreier, B., Luscher, D., Wolfel, J., Gisler, C., Baici, A., Kunz, B. and Sonderegger, P. (2008). Purification and enzymological characterization of murine neurotrypsin. *Protein Expr. Purif.* **61**, 13-21.

Rulicke, T. (2004). Pronuclear microinjection of mouse zygotes. *Methods Mol. Biol.* **254**, 165-194.

Sanes, J. R. and Lichtman, J. W. (2001). Induction, assembly, maturation and maintenance of a postsynaptic apparatus. *Nat. Rev. Neurosci.* **2**, 791-805.

Sauer, B. (1998). Inducible gene targeting in mice using the Cre/lox system. *Methods* **14**, 381-392.

Slater, C. R. (1982). Postnatal maturation of nerve-muscle junctions in hindlimb muscles of the mouse. *Dev. Biol.* **94**, 11-22.

Stephan, A., Mateos, J. M., Kozlov, S. V., Cinelli, P., Kistler, A. D., Hettwer, S., Rulicke, T., Streit, P., Kunz, B. and Sonderegger, P. (2008). Neurotrypsin cleaves agrin locally at the synapse. *FASEB J.* **22**, 1861-1873.

VanSaun, M. and Werle, M. J. (2000). Matrix metalloproteinase-3 removes agrin from synaptic basal lamina. *J. Neurobiol.* **43**, 140-149.

VanSaun, M., Herrera, A. A. and Werle, M. J. (2003). Structural alterations at the neuromuscular junctions of matrix metalloproteinase 3 null mutant mice. *J. Neurocytol.* **32**, 1129-1142.

Weatherbee, S. D., Anderson, K. V. and Niswander, L. A. (2006). LDL-receptor-related protein 4 is crucial for formation of the neuromuscular junction. *Development* **133**, 4993-5000.

Werle, M. J. and VanSaun, M. (2003). Activity dependent removal of agrin from synaptic basal lamina by matrix metalloproteinase 3. *J. Neurocytol.* **32**, 905-913.

Yang, X., Arber, S., William, C., Li, L., Tanabe, Y., Jessell, T. M., Birchmeier, C. and Burden, S. J. (2001). Patterning of muscle acetylcholine receptor gene expression in the absence of motor innervation. *Neuron* **30**, 399-410.